Supplementary Material

High-thermopower ionic thermoelectric hydrogel for low-grade heat harvesting and intelligent fire protection

Zizheng Xiong [a#], Weiguo Wang [a,b#], Zhengzhong Wu [a], Zexi Zhao [a], Qingtao Zeng [a], Hongqiang Li [a], Xingrong Zeng [a*], Bowei Wu [c], Xuejun Lai [a*]

a. School of Materials Science and Engineering, Key Lab of Guangdong Province for High Properties and Functional Polymer Materials, South China University of Technology, No 381, Wushan Road, Tianhe District, Guangzhou 510640, China

b. Guangdong Blue Si&F New Material Co., Ltd, No.43, Electronic Base Factory, Science and Technology West Road, Torch development District, Zhongshan 528437, China

c. The Affiliated High School of South China Normal University, No.1, Zhongshan Ave. West, Tianhe District, Guangzhou 510630, China

#. These authors contributed equally to this work and should be considered co-first authors.

Corresponding Authors:

Prof. Xuejun Lai, E-mail: msxjlai@scut.edu.cn

School of Materials Science and Engineering,

Key Lab of Guangdong Province for High Properties and Functional Polymer Materials,

South China University of Technology,

No 381, Wushan Road, Tianhe District, Guangzhou 510640, China

Tel & Fax: +86-20-22236629

1. Preparation

Tab. S1 The formula of HIG

Samples	AMPSA (g)	AAm (g)	CMC-Na (g)	MBA (mg)	APS (mg)	TEMED (μL)	NaCl (g)	H_2O (g)
HIG0 (n-HIG)	1.5	2.5	0.3	5.0	50.0	40.0	0	10.6
HIG1	1.5	2.5	0.3	5.0	50.0	40.0	0.3	10.3
HIG2	1.5	2.5	0.3	5.0	50.0	40.0	0.5	10.1
HIG3	1.5	2.5	0.3	5.0	50.0	40.0	0.6	10.0
HIG4 (p-HIG)	1.5	2.5	0.3	5.0	50.0	40.0	0.9	9.7
HIG5	1.5	2.5	0.3	5.0	50.0	40.0	1.0	9.6
HIG6	1.5	2.5	0.3	5.0	50.0	40.0	1.2	9.4
HIG7	1.5	2.5	0.3	5.0	50.0	40.0	1.5	9.1
HIG8	1.5	2.5	0.3	5.0	50.0	40.0	2.0	8.6
HIG9	1.5	2.5	0.3	5.0	50.0	40.0	2.5	8.1

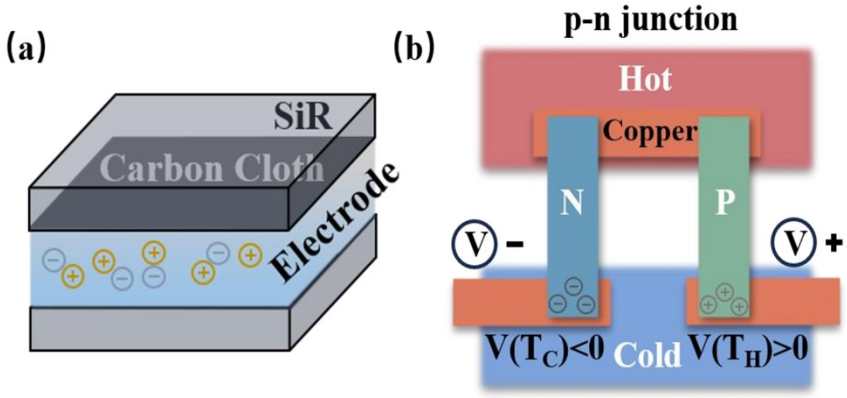

Fig. S1 Structural illustrations of (a) HIG ionic thermoelectric supercapacitor and (b) p-n ionic thermoelectric junction.

2 Characterization

2.1 Fourier transform infrared spectroscopy (FTIR)

The sample flakes were prepared via potassium bromide (KBr) compression method and examined using a Fourier transform infrared spectrometer (TENSOR-27, Bruker, Germany). For each sample, the spectral outcomes were derived on 16 scans with a resolution of 4 cm^{-1} and a scanning range of 4000-400 cm^{-1}.

2.2 Scanning electron microscopy and energy dispersive X-ray spectrometry (SEM-EDS)

The morphology and elemental composition of the hydrogels and the chars after combustion were characterized using a scanning electron microscope (Merlin, Carl Zeiss Jena, Germany) and an energy dispersive X-ray spectrometer (X-MaxN 20, Oxford Instruments, Britain) with an accelerating voltage of 15 kV, together with elemental analysis.

2.3 X-ray photoelectron spectroscopy (XPS)

XPS spectrum was recorded by an X-ray photoelectron spectroscopy (Kratos Axis Ultra DLD, UK) with a Mg Kα monochromatic.

2.4 Mechanical performance test

The samples were cut into long strips with dimensions of 30 mm × 10 mm × 1 mm. Then, the tensile strength and elongation at break were tested using a universal testing machine (Mark-10, US) at room temperature at a tensile speed of 50 $mm \cdot min^{-1}$, and the corresponding stress-strain curves were recorded.

2.5 Flame retardancy test

Vertical burning: Sample (50 mm × 10 mm × 10 mm) was burned with a lamp by using natural gas according to ANSI/UL 94-2010. The distance between wick and the bottom of the sample was 2 cm.

Limiting oxygen index (LOI): LOI value of sample (70 mm × 10 mm × 10 mm) was tested with a JF-3 oxygen index meter (JF3, Nanjing Jiangning Analytical Instrument, China) based on ASTM D2863-09.

Microcombustion calorimeter (MCC): MCC was carried out with a microcombustion calorimeter (Govmark MCC-3, Deatak, USA) according to ASTM D7309. The sample (10-20 mg) was tested from 100 to 600 ℃ at a heating rate of 60 ℃·min^{-1}.

2.6 Thermoelectric performance test

The thermoelectric measurement platform was constructed by employing two Peltiers, thermocouples, coverslips, copper foil electrodes, and a digital multimeter (DMM6500 6 1/2, Keithley Instrument, US), as depicted in **Fig. S2**. The distance between the Peltiers was 30 mm, the contact area between the HIG sample and each Peltiers was 5 mm×10 mm, and one of the Peltiers was powered by a DC power supply to create a temperature difference. In this instance, the size of the HIG sample was 40 mm×10 mm×1 mm.

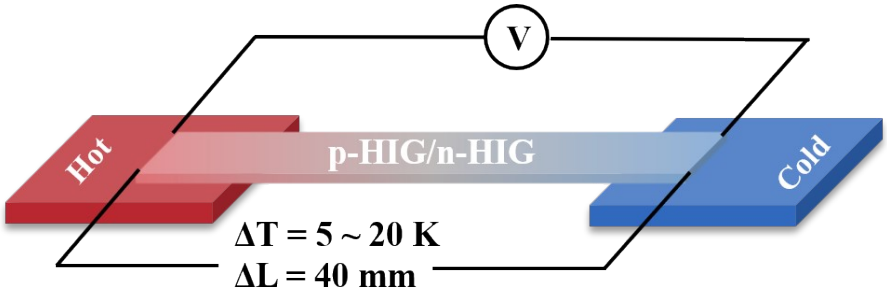

Fig. S2 Schematic diagram of ionic thermovoltage measurement.

2.7 Fire-warning test

The HIG samples (50 mm × 10 mm × 5 mm) were connected to a millivolt signal alarm device (HB414, Dongguan Daxian Instrument Co., Ltd., China) using copper foil electrodes, with the length of the copper foil at both ends of the sample being 5 mm. During the test, the flame of an alcohol lamp was positioned approximately 15 mm from one end of the sample.

The alarm threshold of the millivolt alarm was set at 50 mV. A digital multimeter was used to continuously monitor and record the voltage changes at both ends of the sample, while a video camera captured the entire fire test process. Additionally, for p-HIG, the ignition terminal was connected to the negative terminal of the alarm, whereas for n-HIG, the ignition terminal was connected to the positive terminal of the alarm.

2.8 Thermogravimetry-Fourier transform infrared spectrometry (TG-FTIR)

TG-FTIR spectrometry was tested via a thermogravimeter (STA 449C, Netzsch, Germany) connected with an FTIR spectrometer (Tensor 27, Bruker, Germany). The sample (10-20 mg) was tested from 30 to 800 ℃ at a heating rate of 20 ℃·min^{-1} under air atmosphere.

2.9 Thermogravimetric analysis (TGA)

TGA was performed by using a thermogravimetric analyzer (TGA-209F1, Netzsch, Germany). The sample (5-10 mg) was tested from 30 to 800 ℃ at a heating rate of 20 ℃·min^{-1}.

2.10 Piezoresistive sensing test

The volume resistivity and electrical resistance of the samples were evaluated by using a 4-point probes resistivity measurement system (RTS-9, 4 probes Tech., China) and a digital multi-meter (DMM6500 6 1/2, Keithley Instrument, US).

2.11 Electrochemical measurements

All of the electrochemical measurements were carried out by a Modulab XM electrochemical workstation (Modulab XM, Ametek, US).

Electrochemical impedance spectroscopy (EIS): EIS was performed with the frequency range from 100 to 0.1 kHz, and the ionic conductivity (σ, S·m^{-1}) was calculated according to equation (1):

$$\sigma = \frac{L}{R \times S} \quad (1)$$

where L was the thickness of sample (m), R was the bulk impedance of sample (Ω), and S was the contact area between the electrode (m^2).

Cyclic voltammetry (CV) curve was recorded at a scan rate of 10, 20, 50, 100 and 200 $mV \cdot m^{-1}$, respectively.

Galvanostatic charge-discharge (GCD) curve was obtained at a current density of 0.3, 0.5, 1.0, 1.5 and 2.0 $A \cdot g^{-1}$, respectively, and the specific capacitance (C, $F \cdot g^{-1}$) was calculated according to equation (2):

$$C = \frac{I \times \Delta t}{m \times \Delta V} \quad (2)$$

where I was the discharge current (A), Δt was the discharge time (s), m was the mass of activated carbon in a single electrode and ΔV was the discharge voltage without the voltage drop (V).

3. Results

3.1 Fourier transform infrared spectroscopy (FTIR)

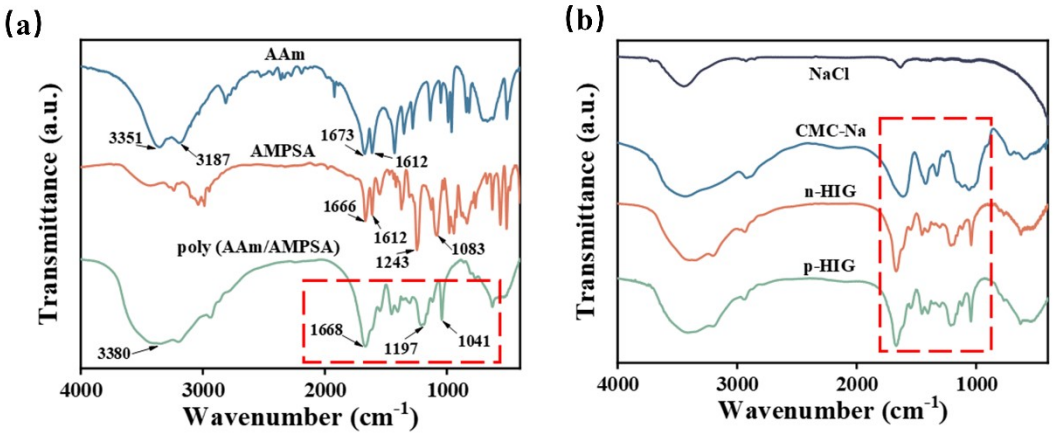

Fig. S3 FTIR spectra of (a) AAm, AMPSA, poly (AAm/AMPSA) and (b) NaCl, CMC-Na, n-HIG, p-HIG

3.2 Mechanical property

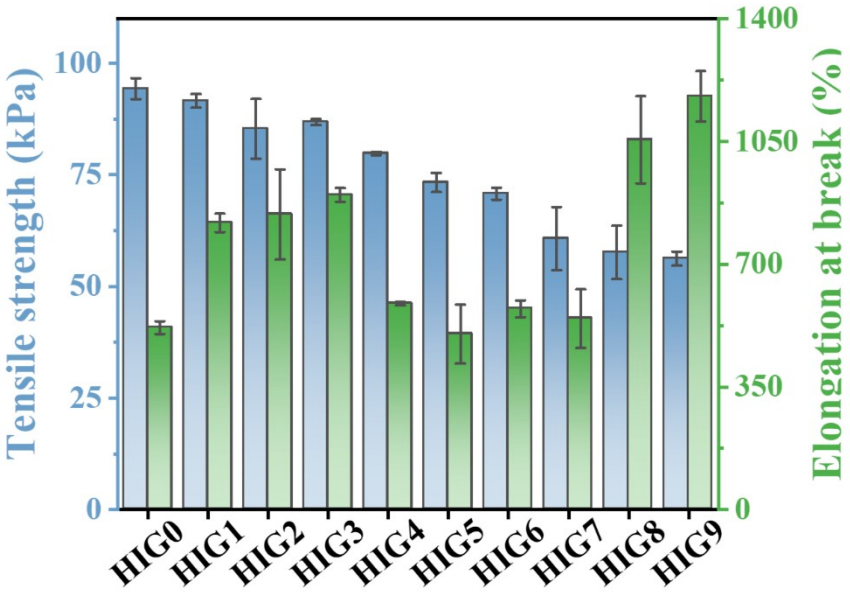

Fig. S4 Tensile strength versus elongation at break for HIG with different NaCl content.

3.3 Thermoelectric properties

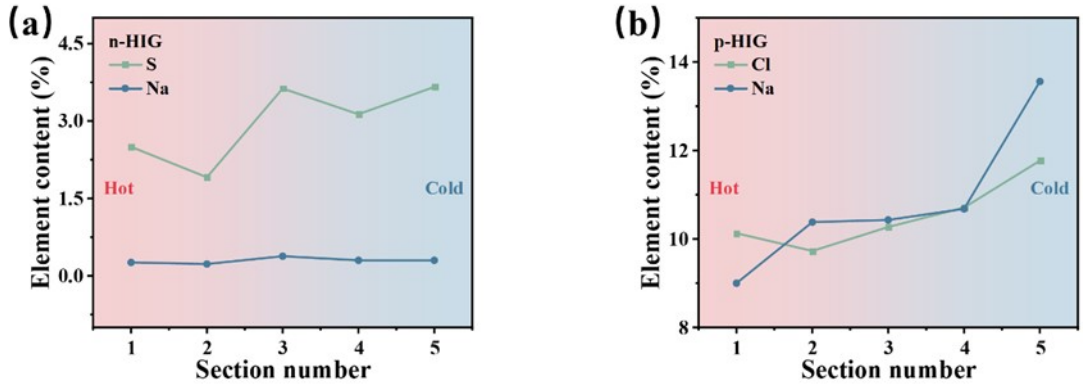

Fig. S5 Ion migration analysis under ΔT=10 K: Cross-sectional elemental distribution in (a) n-HIG and (b) p-HIG.

Tab. S2 The formula of HIG with varying AMPSA content

Samples	AMPSA (g)	AAm (g)	CMC-Na (g)	MBA (mg)	APS (mg)	TEMED (μL)	H_2O (g)
AMPSA0	0.0	2.5	0.3	5.0	50.0	40.0	12.1
AMPSA1	0.5	2.5	0.3	5.0	50.0	40.0	11.6
AMPSA2	1.0	2.5	0.3	5.0	50.0	40.0	11.1
AMPSA3	1.5	2.5	0.3	5.0	50.0	40.0	10.6
AMPSA4	2.0	2.5	0.3	5.0	50.0	40.0	10.1
AMPSA5	2.5	2.5	0.3	5.0	50.0	40.0	9.6

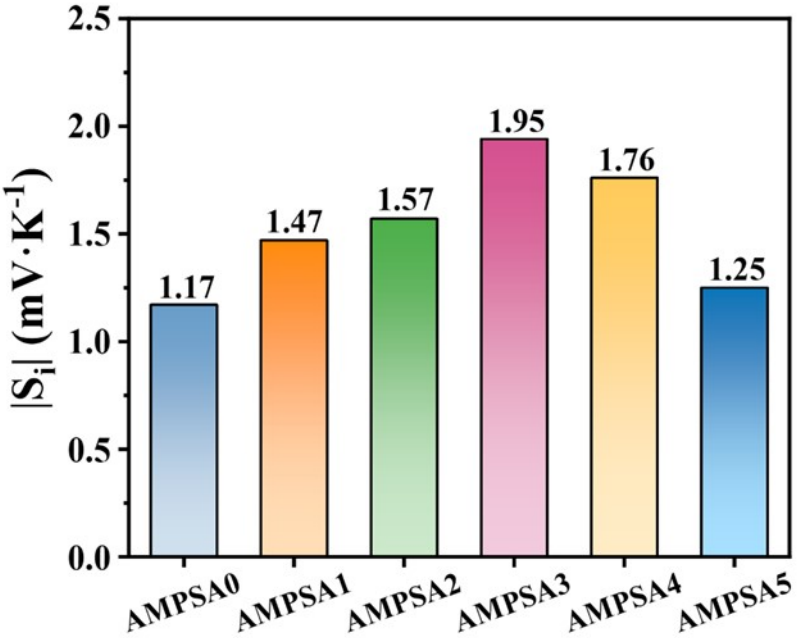

Fig. S6 Seebeck coefficient of HIG with varying AMPSA content.

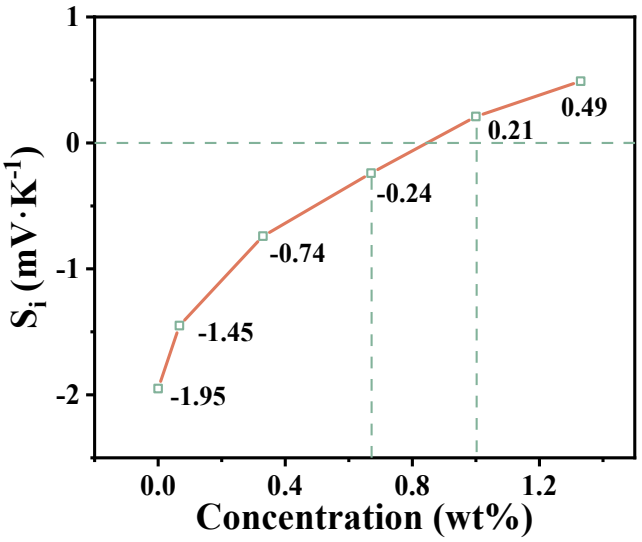

Fig. S7 Ionic Seebeck coefficient for HIG containing trace amount of NaCl.

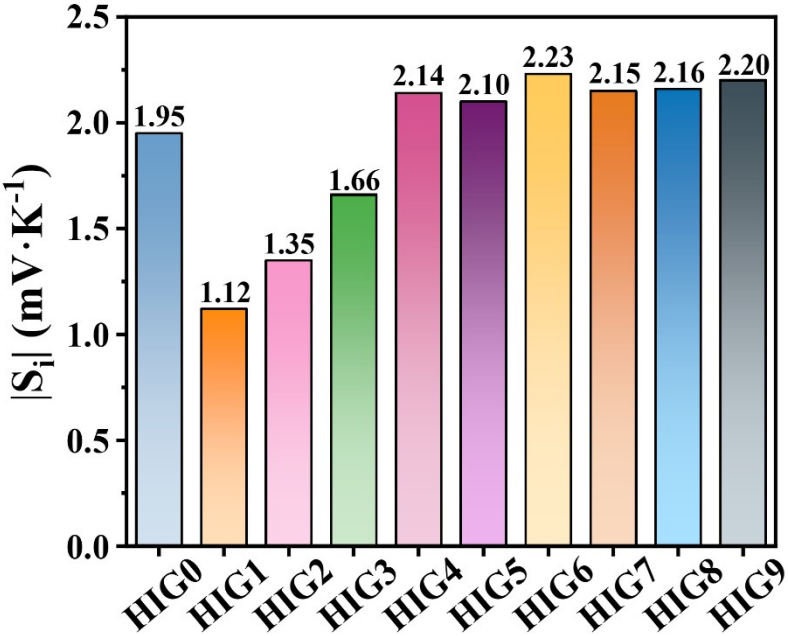

Fig. S8 Seebeck coefficient for HIG with varying NaCl content.

3.4 Flame retardancy

Tab. S3 Flame retardant-related thermal characterization parameters of PAAm, n-HIG, and p-HIG.

Samples	HRC ($J \cdot g^{-1} \cdot K^{-1}$)	PHRR ($W \cdot g^{-1}$)	THR ($W \cdot g^{-1}$)	Temperature (℃)
PAAm	382	318	21	347
n-HIG	267	269	15	371
p-HIG	254	256	15	376

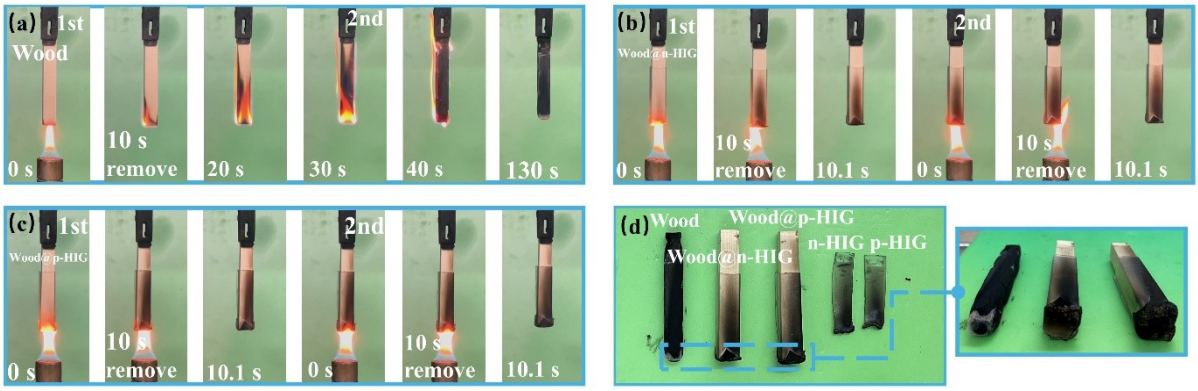

Fig. S9 Video screenshots of the vertical combustion test of (a) Wood; (b) Wood@n-HIG; (c) Wood@p-HIG; (d) Digital photos of the samples after vertical combustion test.

3.5 Thermal capacitance

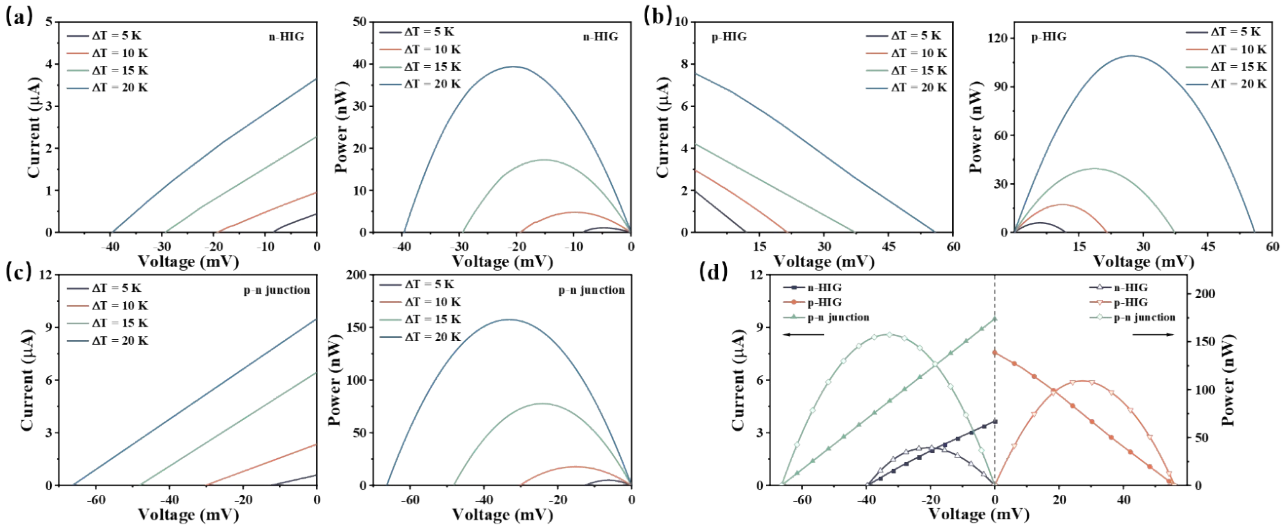

Fig. S10 Current-voltage curves and power-voltage curves of (a) n-HIG; (b) p-HIG and (c) p-n junction thermoelectric capacitor under different ΔT; (d) Comparison of current-voltage curves and power-voltage curves of the thermoelectric capacitors under ΔT = 20 K.

3.6 Tensile sensing properties

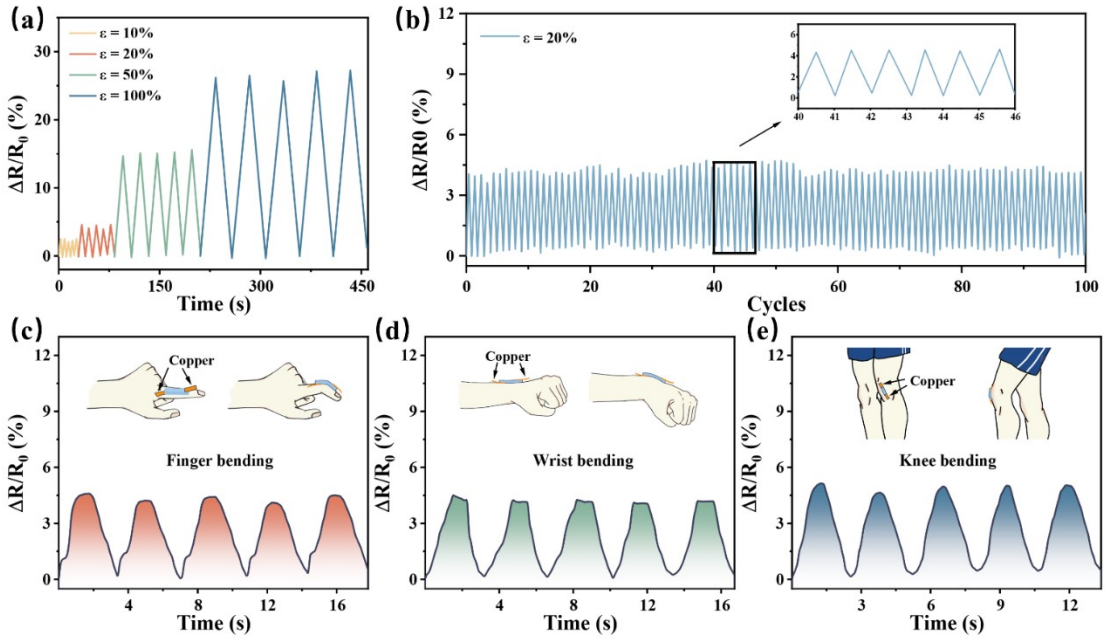

Fig. S11 Resistance response curves of p-HIG at (a) 50 mm·min^{-1} tensile rate at different strain and (c) dynamic resistance responses curve of p-HIG at a strain of 20% with 100 cycles; The resistance response curves of p-HIG in (c) finger bending; (d) wrist bending; (e) knee bending.

3.7 Electrochemical and thermal charging properties of HIG SC

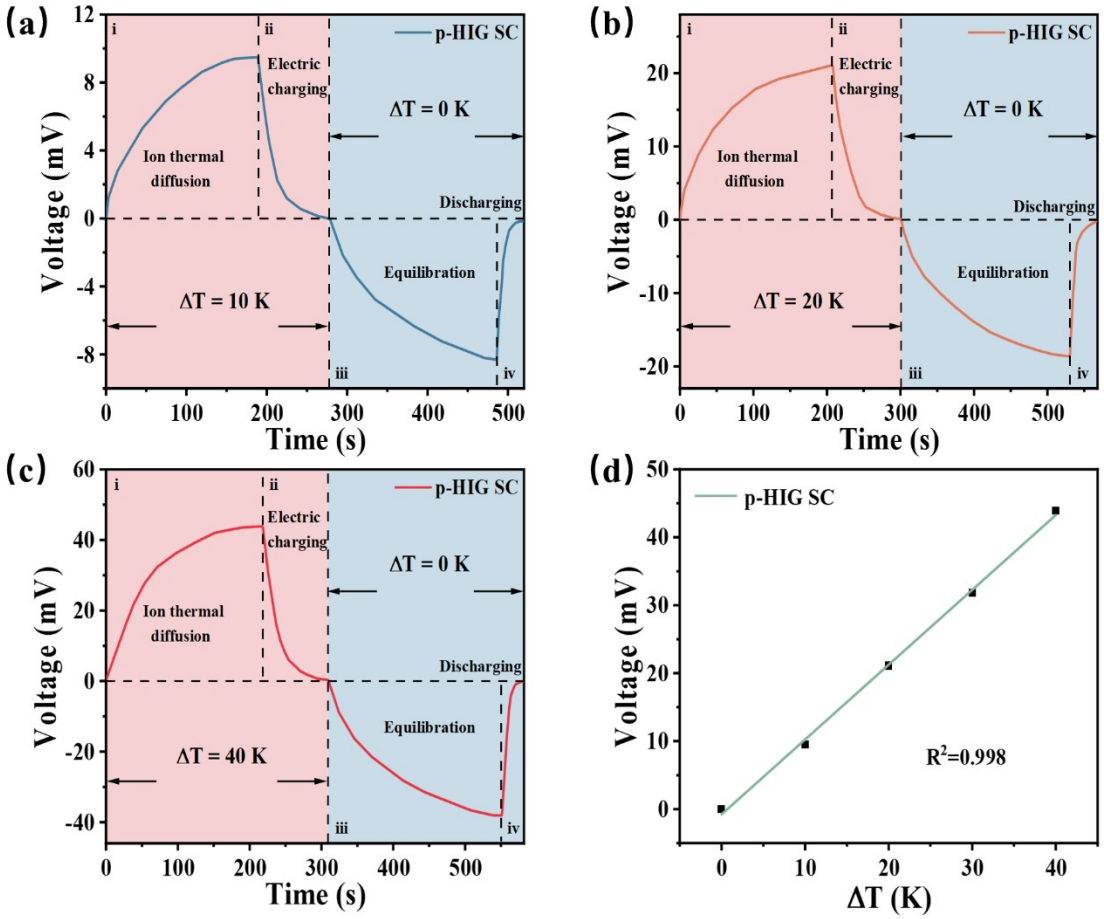

Fig. S12 Thermal charging curves of p-HIG SC at (a) 10 K; (b) 20 K; (c) 40 K; (d) The maximum thermal voltage varied with the temperature difference when the temperature difference of p-HIG SC is 0-40 K.